



Guenov, M. D., Chen, X., Molina-Cristobal, A., Riaz, A., van Heerden, A. S. J. and Padulo, M. (2018) Margin allocation and tradeoff in complex systems design and optimization. *AIAA Journal*, 56(7), pp. 2887-2902. (doi: [10.2514/1.J056357](https://doi.org/10.2514/1.J056357))

There may be differences between this version and the published version. You are advised to consult the publisher's version if you wish to cite from it.

<http://eprints.gla.ac.uk/223562/>

Deposited on 2 October 2020

Enlighten – Research publications by members of the University of Glasgow  
<http://eprints.gla.ac.uk>

# Margin Allocation and Trade-off in Complex Systems Design and Optimization

---

Marin D. Guenov, Xin Chen, Arturo Molina-Cristóbal, Atif Riaz, Albert S.J. van Heerden  
*Centre for Aeronautics, Cranfield University, Cranfield, Bedfordshire, MK43 0AL, United Kingdom*

and

Mattia Padulo

*Airbus S.A.S., 1 Round Point Maurice Bellonte, 31707 Blagnac, France*

**Presented is an approach for interactive margin management. Existing methods enable a fixed set of allowable margin combinations to be identified, but these have limitations with regard to supporting interactive exploration of the effects of: 1) margins on other margins, 2) margins on performance and 3) margins on the probabilities of constraint satisfaction. To this purpose, the concept of a margin space is introduced. It is bi-directionally linked to the design space, to enable the designer to understand how assigning margins on certain parameters limits the allowable margins that can be assigned to other parameters. Also, a novel framework has been developed. It incorporates the margin space concept as well as enablers, including interactive visualization techniques, which can aide the designer to explore the margin and design spaces dynamically, as well as the effects of margins on the probability of constraint satisfaction and on performance. The framework was implemented into a prototype software tool, AirCADia, which was used for a qualitative evaluation by practicing designers. The evaluation, conducted as part of the EU TOICA project, demonstrated the usefulness of the approach.**

## Nomenclature

$AR$  = aspect ratio  
 $W_f$  = fuel mass [ $lb$ ]  
 $W_p$  = payload mass [ $lb$ ]  
 $W_e$  = empty weight [ $lb$ ]  
 $W_0$  = take-off weight [ $lb$ ]  
 $LoD$  = lift-over-drag  
 $ESAR$  = equivalent still-air range [ $nm$ ]  
 $TOFL$  = take-off field length [ $ft$ ]  
 $Mach$  = Mach number  
 $a$  = speed of sound [ $kts$ ]  
 $SFC$  = specific fuel consumption [ $lb/(hr \cdot lbf)$ ]  
 $SLST$  = sea level static thrust [ $lbf$ ]  
 $S_{ref}$  = wing reference area [ $ft^2$ ]  
 $C_{L_{to}}$  = take-off lift coefficient

# 1. Introduction

The ever-increasing drive for competitive robustly designed products has led to the growing importance of uncertainty quantification and management (UQ&M) in both academia and industry. One specific aspect of this wider field, which has motivated the research presented in this paper, is margin management. Margins can be viewed as ‘reserves’ which are placed on variables of interest, such as performance constraints, to account for uncertainties (and/or unknowns) which are expected to affect the accurate prediction of these variables. The uncertainties can be associated with computational means (e.g. accuracy or bias of computational models), manufacturing tolerances, and/or operational conditions. Assigning margins may also be used as a means of ensuring product upgradeability, or to reduce the risk of underperformance or even failure. In any case, using margins excessively could result in overdesigned and potentially less competitive products. This is of particular concern in the aircraft manufacturing industry, where every pound of extra weight counts. ‘Over-conservatism’ can further be exacerbated through cumulative effects (i.e. adding margins on parameters that already have margins), due to the hierarchical and distributed nature of complex product development, where each team (discipline) would have their specific reasons for assigning higher margins on their share of the work.

As an example, consider the following illustrative scenario: During the design of a new aircraft, the designers (also referred to in this paper as ‘architects’, or ‘systems architects’) may need to plan for the possible evolution of (market) requirements, such as expected growth in the number of passengers (resp. fuselage size), in addition to the need to comply with performance constraints (e.g., allowable take-off and landing distance, acceptable temperature, pressure and air quality in the cabin, and so forth). Uncertainties associated with these parameters can be accounted for by introducing margins. The systems architects would ideally like to be able to negotiate (trade off) these margins across and between the systems and the sub-systems levels of the product decomposition, to ensure design feasibility. For example, given a violation of a thermal constraint, the architect may wish to reduce, if possible, the electrical load margins on certain electrical components, if that would make the thermal loads on particular structural elements acceptable. In such a way, integration problems, or in the worst case, a major redesign effort may be avoided.

The research presented in this paper constitutes a contribution to tackling these margin-related challenges, as formulated by the European project TOICA (Thermal Overall Integrated Conception of Aircraft) [1],[2]:

- “To better anticipate changes in the specifications from other disciplines and/or partners”.
- “To develop better [interactive] trade-offs and adequate risk mitigations taking into account the current level of quality of the results”.
- “To improve the margin policy definition” (i.e. to develop capabilities to manage margins during development to meet targets improving the management of the margin policy).

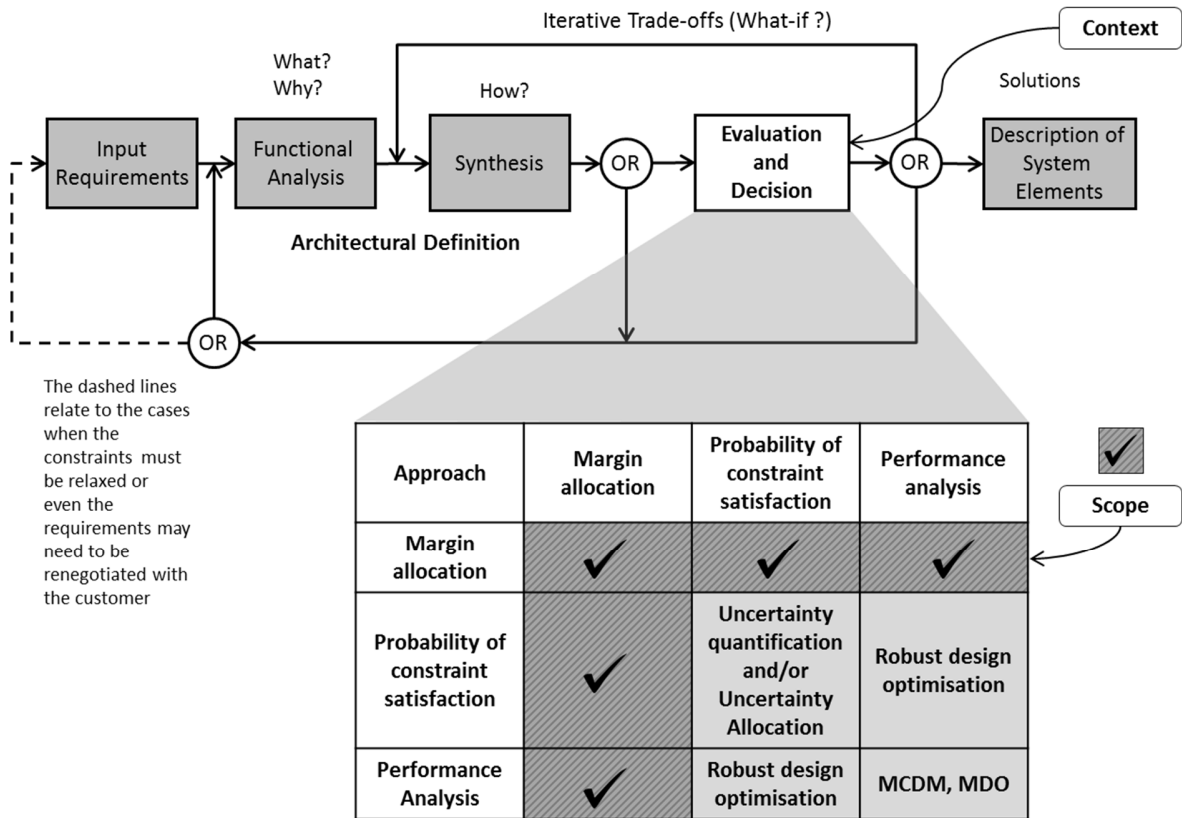


Fig. 1 Context and scope of the proposed work (context diagram adapted from Ref. [3]).

Within this context, the overall aim of our research has been to develop methods and tools for margin management and trade-offs within and across product decomposition boundaries. The scope of the work is restricted to the ‘evaluation and decision’ step of the systems engineering process (Fig. 1). In this step, multiple designs are usually analyzed to determine which of them best satisfies the requirements. Such analyses may involve different types of trade-off studies. Some of these (shown in grey in the lower part of Fig. 1) belong to relatively well-understood topics and are not covered further in this paper.

In the current work, the focus is on three types of trade-off studies related specifically to margins (marked by the ticks in Fig. 1). As discussed above, assigning margins arbitrarily can adversely affect system performance. Therefore, it is vital to find an appropriate balance between margins, expected performance, and risk. There are existing methods which are able to find a fixed set of allowable margin combinations [4],[5], but these appear to be limited with regard to supporting interactive exploration of the effects of: 1) margins on other margins, 2) margins on performance and 3) margins on the likelihood of constraint satisfaction. Thus, there is a need for an interactive framework, making these types of trade-offs explicit. This is important, not least because it enhances the ability of the designer to interactively allocate margins and swiftly view the potential effects during the early design stages.

In this regard, there are two major objectives in this paper, formulated to meet the requirements stipulated by the industrial stakeholders of the TOICA project (see above). The first one is to integrate the concepts of deterministic margin allocation and probabilistic constraint satisfaction in an interactive margin-management framework accounting for:

- evolving design requirements (i.e. changeable constraints);
- margins on design variables, parameter variations and model uncertainty;
- trade-offs between margins and probability of constraint satisfaction;
- margin trade-offs at the same or between different product decomposition levels.

As indicated above, such a framework is expected to enable the designer to interactively explore a single design concept, for example, when trying to find a compromise solution in the face of a potentially significant redesign effort, to deal with evolving (e.g. changing requirements), rather than fixed design options, or to identify a set of promising robust solutions. This will ultimately allow for more design freedom (flexibility) during the conceptual design process.

The second, practical, objective was to demonstrate the usefulness of such a framework to practicing aircraft designers and architects, within the scope of model-based computational design, as part of the European project TOICA, as will be elaborated upon later.

The rest of the paper is organized as follows: the next section outlines some basic concepts, state of the art tools and enabling methods related to the presented work. The proposed method is described in Section III. The demonstration of the proposed approach, implemented in a prototype software tool as part of the TOICA project, is presented in Section IV. Finally, conclusions are drawn and future work is outlined in Section V.

## 2. Background

Outlined in this section are basic concepts, assumptions and enabling methods related to and utilized in the proposed framework.

### 2.1. Computational workflow

In this paper, the scope is restricted (but not limited) to the model-based design approach, where a set of models are used to evaluate performance. The models are assembled into a computational workflow with inputs specified by the user and where all dependent variables (the outputs) are calculated automatically [6]. Such a computation can be represented in the form of a function, as follows:

$$\mathbf{Y} = F(\mathbf{X}) \quad (1)$$

where,

$\mathbf{X} = (x_1, x_2, \dots, x_l) \in \mathbb{R}^l$  is a vector of  $l$  input variables (simply referred to as inputs), and

$\mathbf{Y} = (y_1, y_2, \dots, y_m) \in \mathbb{R}^m$  is a vector of  $m$  output variables.

$F$  denotes the computational workflow, comprised by the constituent models.

An illustrative example of a computational workflow is shown in Fig. 2. It represents a simple aircraft sizing code based on text-book equations [7],[8]. For convenience, this workflow will be referred to as ‘SIMPCODE’ for the remainder of the paper. The assumptions of the example are given in Table 1. In Fig. 2 the white ovals denote the input variables  $\mathbf{X}$ , including:  $AR$ ,  $W_f$ , and  $W_p$ ; the grey ovals represent the performance outputs,  $\mathbf{Y}$ , which include:  $LoD$ ,  $W_e$ ,  $W_0$ ,  $ESAR$ , and  $TOFL$ .

Table 1 SIMPCODE parameter values.

Paramete	value
$Mach$	Mach number = 0.85
$a$	Speed of sound = 576.419 knots at 35
$SFC$	Specific fuel consumption = 0.6 lb/hr/lb
$SLST$	Sea level static thrust = 54 000 lb
$S_{ref}$	Wing reference area = 1 360 ft <sup>2</sup>
$C_{L_{to}}$	Take-off lift coefficient = 2.1
<b>Constrain</b>	
$ESAR$	equivalent still-air range $\leq 3500$ nm

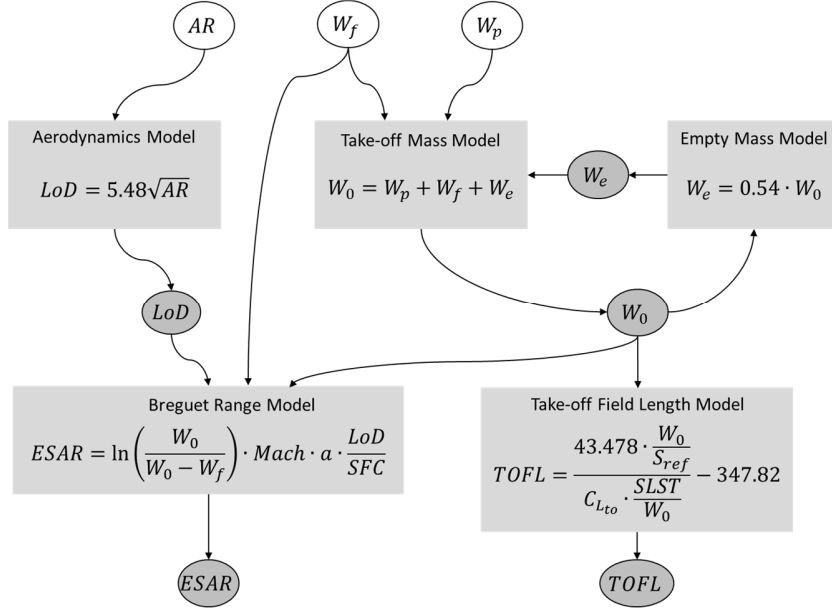


Fig. 2 Example of a simple aircraft sizing workflow.

Fig. 2 represents the workflow of SIMPCODE in its default state, that is, the default inputs to the individual constituent models are preserved. Depending on the study, the designer may choose to designate some of the default outputs as inputs (independent variables). In this case the workflow needs to be dynamically “reversed” using numerical methods [6].

## 2.2. Design space exploration

In the computational context of this work, a design space ( $DS$ ) is defined as the hypercube confined by the specified (valid) ranges of all design variables. The specified (valid) range of the  $i$ th design variable,  $DV_i$ , is given as follows:

$$DV_i = \begin{cases} [dv_i^{LB}, dv_i^{UB}], i = 1, \dots, r; & \text{for continuous variables} \\ \{dv_1, dv_2, dv_3, \dots, dv_{r_i}\}; & \text{for discrete variables} \end{cases} \quad (2)$$

where  $dv_i \in DV_i$  lies between a lower-bound ( $dv_i^{LB}$ ) and an upper-bound ( $dv_i^{UB}$ ),  $r$  is the number of design variables and  $r_i$  represents the number of options for the  $i$ th (discrete) design variable. Without loss of generality, it is assumed here that the design variables are continuous. Then, the  $DS$  can be represented by Eq. (3), as the Cartesian product of all the design variable sets ( $DV_i, \forall i = 1, \dots, r$ ). Each element in the  $DS$  is a possible design solution, i.e., an ordered  $r$ -tuple  $(dv_1, dv_2, \dots, dv_r)$ , where  $dv_1$  belongs to  $DV_1$ ,  $dv_2$  belongs to  $DV_2$  and so forth.

$$DS = DV_1 \times DV_2 \times \dots \times DV_r \quad (3)$$

### 2.2.1. Design space sampling techniques

The *DS* for continuous design variable sets contains an infinite number of possible design solutions. Therefore, sampling techniques are usually employed to enumerate and evaluate a selected subset of design solutions. A Design of Experiments (DoE) study [9] is a statistical technique for sampling the design space in a systematic way.

### 2.2.2. Iso-contours plots

A constraint analysis method, based on iso-contours [10], is another enabler for design space exploration. In this method, following a full factorial sampling (FFS) and the corresponding execution of the computational workflow for each design point, the multi-dimensional design space is divided into multiple 2D projections or slices (contour plots). These show the iso-contour lines of the performance constraints for any two design variables, assuming all other design variables remain constant.

### 2.2.3. Parallel coordinates plots

The parallel coordinates plot (PCP) [11],[12] allows visualization of high-dimensional spaces, where each design solution is represented as a polyline with vertices on the (parallel) vertical axes. In addition to visualizing multiple parameters together, the PCP is useful for interactive filtering of solutions based on specified criteria.

## 2.3. Design margin definition

In various contexts, margins could be introduced either in project budgets, schedules, or technical performance parameters (e.g. mass, power consumption, etc.) [13]–[16]. Only margins related to technical performance are considered here.

Several definitions of a margin can be found in the literature. For example, a margin renders a design “more capable” than “necessary” [13] and “...intuitively, a margin is a measure of the difference between a requirement placed on the performance of a system and the predicted performance of the system...” [17]. Another definition of margins is that they are “variations in design parameters measured relative to worst-case expected values” and can be expressed mathematically as “a percentage difference between the ‘worst-case estimate’ (WCE) and ‘current best estimate’ (CBE)” [14]. Note that the above definitions are conceptually equivalent when the requirement equals the worst-case estimate.

WCE will be referred to in this paper as a ‘conservative value’ ( $z_C$ ) and CBE as a ‘nominal value’ ( $z_N$ ). The margin can therefore be formulated either as an absolute value, or, equivalently, as a percentage, as follows:

$$\begin{aligned} Mar &= z_C - z_N && \text{Margin as an absolute value} \\ \%Mar &= [(z_C - z_N) / z_N] * 100 && \text{Margin as a percentage} \end{aligned} \quad (4)$$

The implications of placing margins on the variables in a computational workflow are discussed next, by making use of SIMPCODE (Fig. 2), where  $AR$ ,  $W_f$ , and  $W_p$  are independent input variables, whereas



*ESAR* and *TOFL* are computational outputs. *LoD* and  $W_0$  are ‘intermediate variables’ and could be treated either as input or output variables.

Margins could be applied to any of these variables for two main reasons:

- Margins accounting for evolving design requirements: these could be allocated on design or performance parameters to enhance flexibility, i.e., accounting for the possibility that requirements may change with time (both during and/or beyond the development phase of the product). In other words, providing margins may offer reserves that could allow for the future evolution of the product (system). Note that margins accounting for evolving requirements could be implemented on input variables or on the constraints of output variables. For example, considering SIMPCODE, a margin could be applied on the payload mass,  $W_p$  (an input variable and design parameter), to cater for the possibility that the required payload may increase during the product development process (or later, in the case of a derivative product). Similarly, a margin could be placed on the required take-off field length, *TOFL*, in anticipation of a change towards a lower maximum acceptable value (due to, for example, airlines wanting to operate from shorter runways).
- Margins accounting for model uncertainty: a margin could be allocated if it is believed that the estimate of a particular performance value is optimistic, which could arise due to the model(s) not being sufficiently accurate. For example, referring again to the SIMPCODE example, a margin could be applied to the equivalent still-air range (*ESAR*), to account for uncertainty in the inputs to the Breguet-Range model. Margins accounting for model uncertainty are applied to the output variables of the computational models.

The relationship between margins, uncertainty, and the probability of constraint satisfaction has been recognized in the literature (e.g. [14]). This relationship is illustrated by two possible design scenarios.

In the first scenario, the margin is specified a priori, based on experience, or on historical data (see, e.g., [4],[5]). By using this margin, as well as the results from an uncertainty quantification study, the decision maker would be able to assess the probability of constraint satisfaction as a consequence of setting (allocating) this margin. Scenario 1 can be formulated mathematically as follows in the deterministic case:

$$y_N \leq R_y - Mar. \quad (5)$$

Here,  $y_N$  is the nominal value of a performance output obtained from a model (workflow) calculation, and  $R_y$  is the requirement (constraint) placed on this output. As Eq. (5) shows, the constraint becomes harder to satisfy after the margin, *Mar*, is allocated.

Next, assume that, uncertainty affecting the output variable  $y$  follows a statistical distribution and its probability density function (PDF) can be represented as  $f_y$  (Fig. 3). The probability of constraint satisfaction (represented by the white area under the curve defined by  $f_y$ ) is then:

$$Pr(y \leq R_y) = \int_{-\infty}^{R_y} f_y(y) dy = F_y(y_N + Mar), \quad (6)$$

where  $R_y = y_N + Mar$  and  $F_y$  is the Cumulative Density Function (CDF). Provided that the PDF,  $f_y$ , is known, the probability of satisfaction can be formulated as a function of the magnitude of the margin.

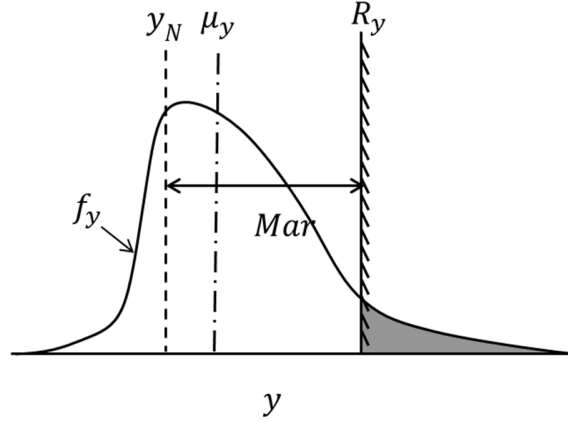


**Fig. 3 The relationship between probability of constraint satisfaction and margin.**

In the second scenario, the designer may specify a required probability of constraint satisfaction and perform an uncertainty quantification study to determine a reasonable size of the margin (see, e.g., [14]–[16]). This could be achieved by the margin relation in Eq. (7):

$$Mar = F_y^{-1}(Pr) - y_N, \quad (7)$$

where  $F_y^{-1}$  is the inverse CDF.

This scenario has been studied also in the area of mechanical failure probability (load-strength interference) [18]. However, the intended application of the proposed method is predominantly to support the investigation of design feasibility. Therefore, these types of in-service operational “safety/reliability” margins, where the probability of failure is required to be very low, are considered outside the scope of this paper.

### 3. Proposed Framework

Presented in this section is the proposed framework for design margin allocation and trade-off. First, the concept of a margin space ( $MS$ ) and its relation to the design space ( $DS$ ) is introduced. The second part of the section introduces the proposed techniques for margin trade-offs.

#### 3.1. Margin space ( $MS$ )

Similar to the definition of a design space ( $DS$ ), a margin space ( $MS$ ) is a hypercube defined by the ranges of all considered (allocated) margins. The design variables are assumed to be independent. The same assumption applies to the margin variables. The  $MS$  is constructed starting with a choice of interval values within a defined lower and upper bound for each margin. The general form of the interval of the  $k$ th margin ( $Mar_k$ ) is given by Eq. (8), where  $S_k$  represents the set of values considered for the  $k$ th margin, and  $n$  is the total number of margins.  $Mar_k^{LB}$  and  $Mar_k^{UB}$  represent the lower and upper limit values for the  $k$ th margin, respectively.

$$S_k = [Mar_k^{LB}, Mar_k^{UB}] = \{ Mar_k \mid Mar_k^{LB} \leq Mar_k \leq Mar_k^{UB} \}, \quad k = 1, 2, \dots, n \quad (8)$$

After specifying the intervals  $S_k$  for each margin,  $Mar_k$ , the  $MS$  is generated by obtaining the Cartesian product of all the margin intervals,  $S_k$ . Each element in the  $MS$  is the ordered  $n$ -tuple  $(Mar_1, Mar_2, \dots, Mar_n)$ , where  $Mar_1$  belongs to  $S_1$ ,  $Mar_2$  belongs to  $S_2$  and so forth. In the present work, the ordered  $n$ -tuple of the values of the margins is referred to as a ‘margin combination’. The general form of the  $MS$  is given by Eq. (9). It is important to note that if the number of margins,  $n$ , is large, a sensitivity analysis study could be performed to select a few most influential ones.

$$MS = S_1 \times S_2 \times \dots \times S_n = \{ (Mar_1, Mar_2, \dots, Mar_k, \dots, Mar_n) \mid Mar_k \in S_k \} \quad (9)$$

Referring to SIMPCODE as an example, consider the margins on Lift-to-Drag Ratio ( $Mar_{LoD} = Mar_1$ ), Empty Weight ( $Mar_{We} = Mar_2$ ), and Payload Weight ( $Mar_{Wp} = Mar_3$ ).  $Mar_{Wp}$  is applied to a representative nominal value for payload weight of 28 000 *lb*, whereas  $Mar_{We}$  and  $Mar_{LoD}$  are applied to the relevant model outputs. Intervals can be specified on these margins, for example,  $S_{LoD} = S_1 = [0, 5]\%$ ,  $S_{We} = S_2 = [0, 5]\%$ , and  $S_{Wp} = S_3 = [0, 10]\%$ , respectively. The  $MS$  can subsequently be obtained as follows:

$$MS = S_{LoD} \times S_{We} \times S_{Wp} = [0,5]\% \times [0,5]\% \times [0,10]\% \quad (10)$$

The  $MS$  obtained in Eq. (10) contains an infinite number of combinations of the three margins, so enumerating and evaluating every point in the  $MS$  is infeasible. Furthermore, multiple combinations from the  $MS$  may be considered equivalent from the designer’s point of view. Therefore, for practical purposes only a subset (sample) of the combinations from the  $MS$  needs to be evaluated. This can be obtained through a FFS. The resulting subset of the  $MS$ , represented as  $MS^d$ , can be obtained by discretizing the considered intervals of the margins and then taking the Cartesian product of the discretized margin intervals. The general form of  $MS^d$  is given by Eq. (11), where  $S_k^d$  represents the discretized interval of the  $k$ th margin.

$$MS^d = S_1^d \times S_2^d \times \dots \times S_k^d \times \dots \times S_n^d \quad (11)$$

Considering SIMPCODE, assume that the three margins are discretized into six equidistant values each, i.e.,  $S_{LoD}^d = \{0,1,2,3,4,5\}\%$ ,  $S_{We}^d = \{0,1,2,3,4,5\}\%$ , and  $S_{Wp}^d = \{0,2.5,5,7.5,10\}\%$ . The discretized margin space  $MS^d$  can subsequently be obtained as follows:

$$MS^d = S_{LoD}^d \times S_{We}^d \times S_{Wp}^d = \{0,1,2,3,4,5\}\% \times \{0,1,2,3,4,5\}\% \times \{0,2.5,5,7.5,10\}\% \quad (12)$$

The  $MS^d$  in Eq. (12) consists of  $6 \times 6 \times 5 = 180$  margin combinations. Each margin combination is created by taking one value from each  $S_k^d$ . For example, one of these combinations, the 3-tuple (3%, 2%, 7.5%) indicates that the selected values for  $Mar_{LoD}$ ,  $Mar_{We}$ , and  $Mar_{Wp}$ , are 3%, 2%, and 7.5%, respectively.

Some of the margin combinations from the  $MS^d$  may not be feasible because of the resulting performance not meeting the performance constraints. A margin combination in the margin space is feasible if it satisfies the condition given by Eq. (13), where  $p$  is the number of performance constraints and  $n$  is the number of design margins.

$$\mathbf{C} = \{ \mathbf{M} \mid G_i(\text{DP}, \mathbf{M}) - g_i \leq 0; \forall i = 1, 2, \dots, p \} \quad (13)$$

where  $\mathbf{C}$  is the set of feasible margin combinations,  $\mathbf{M} = (Mar_1, Mar_2, \dots, Mar_n)$  is the vector of a particular magnitudes for each of the margins, DP is the selected design point at value  $(dv'_1, dv'_2, \dots, dv'_r)$ , and  $g_i$  represent the  $i$ th constraint. Note that the condition in Eq. (13), i.e.,  $G_i(\text{DP}, \mathbf{M}) - g_i \leq 0$ , corresponds to the case when the constraint is ‘lower the better’. For ‘the higher the better’ type constraints, the condition will be,  $G_i(\text{DP}, \mathbf{M}) + g_i \leq 0$ .

It is important to note that, although  $MS^d$  will be common for all the points in the design space, the feasible  $MS^d$  may be different for each design solution (point). In other words, a feasible margin space is linked to a particular point in the design space. This is demonstrated in Fig. 4, where the SIMPCODE design space is shown, along with two selected design points, DP1 and DP2, and the corresponding margin spaces. Here, the two design variables considered are  $x_1$ -aspect ratio ( $AR$ ) and  $x_2$ -fuel mass ( $W_f$ ) with bounds  $[8, 9]$  and  $[35000, 37000]$   $lb$ , respectively. The feasible margin spaces in Fig. 4 are indicated by the white regions, bounded by the iso-contours representing the aircraft range constraint ( $ESAR \leq 3500nm$ ). Fig. 4b shows the  $MS$  for design point DP1. It can be seen that if design point DP2 is selected in the design space (Fig. 4a), the feasible (allowable) margin space gets reduced, as shown in Fig. 4c. Note that, for simplicity, only one iso-contour ( $ESAR \leq 3500nm$ ) is shown in Fig. 4. Introducing iso-contours for other constraints may further constrict the margin spaces. This will be illustrated in the evaluation section.

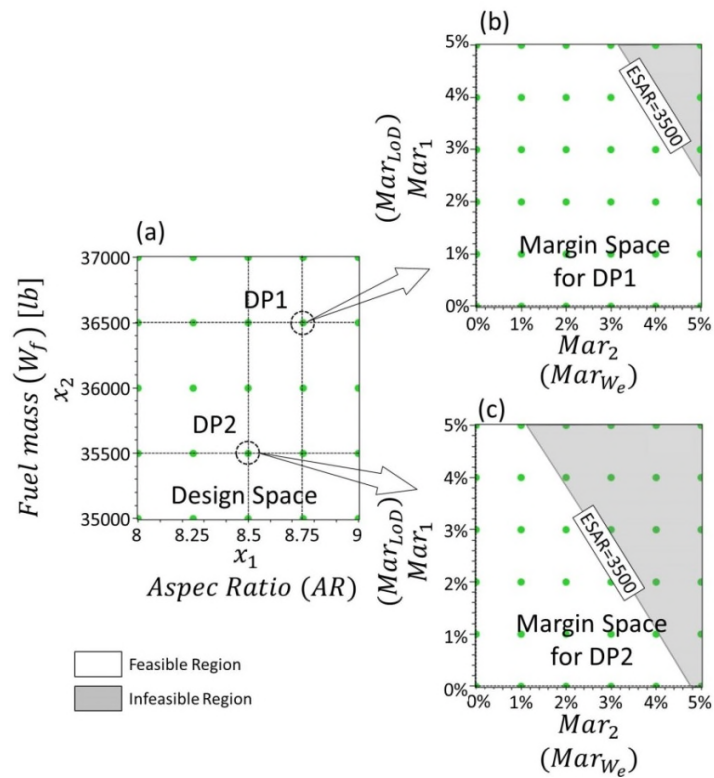


**Fig. 4** Effect of design point selection on the margin space.

Similarly, if a margin combination is selected in the margin space ( $MS$ ), the feasible design space changes. This is illustrated in Fig. 5, again using SIMPCODE. Fig. 5a shows the design space with zero margins. Selection of a margin combination, represented by the dotted circle in Fig. 5b, modifies the feasible design space, as shown in Fig. 5c.

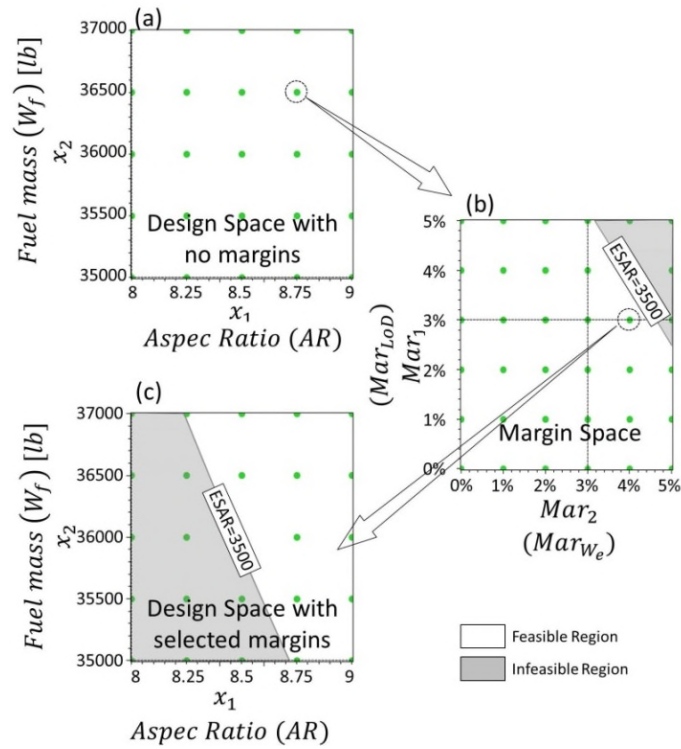


Fig. 5 Effect of margin selection on the design space.

The explicitly defined and bi-directionally linked margin and design spaces constitutes one of the central concepts of this research and is intended to enable interactive trade-offs between risk mitigation and design performance, as elaborated below.

### 3.2. Margin trade-off techniques

In this section, techniques for three types of margin trade-offs are presented (refer also to Fig. 1). It is important to note that in practice these trade-offs can be conducted in any order, subject to available information. Also, it should be noted that the sequence of the trade-offs may lead to different sets of design candidates. The advantage of an interactive framework, such as the one proposed here, is to enable the designer to investigate the effects of selecting alternative sequences.

#### 3.2.1. Margin vs. margin trade-offs

When margins are allocated on selected parameters of a given parameter set, the allowable maximum margin values on the other parameters of the set are reduced, due to the presence of performance constraints linking the parameters. It is therefore necessary to conduct a trade-off study to find acceptable margin combinations that satisfy all the constraints. In this subsection, two techniques are proposed to support this type of trade-off study – ‘intra margin space investigation’ and ‘deterministic design band filtering’. Intra margin space investigation can be used to explore how changing the allowable margin on one parameter affects the allowable margins on other parameters, whereas deterministic design band filtering is useful when the designer seeks to maintain minimum values for the margins.

### 3.2.1.1. Intra margin space (MS) investigation

Given a single design point, selecting particular values for one or more of the margins may cause the maximum allowable values for the remaining margins to change. It is therefore desirable to be able to explore the effects of selecting specific combinations within the feasible margin space associated with a particular design point.

For such an exploration, it is proposed to use a matrix of two-dimensional contour plots of the margin space (MS). An illustration of how this matrix can be used is shown in Fig. 6, using SIMPCODE as a simple example. The matrix shows all three combinations of the MS contour plots (i.e.  $Mar_1$  vs.  $Mar_2$ ,  $Mar_1$  vs.  $Mar_3$ , and  $Mar_2$  vs.  $Mar_3$ ). The MS matrix shown in Fig. 6 corresponds to the selected design point, DP1 in Fig. 4. For the selected margin combination point, MP1 ( $Mar_1 = 1\%$ ,  $Mar_2 = 3\%$ ,  $Mar_3 = 0\%$ ), the iso-constraint lines for the aircraft range (ESAR = 3500nm) are shown in each of the three contour plots.

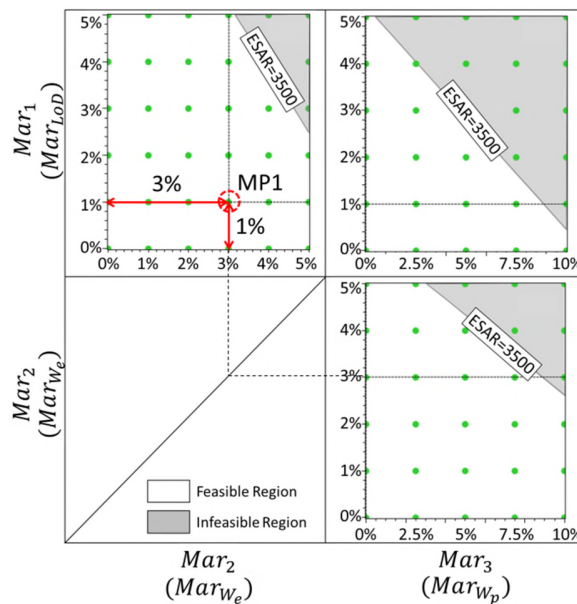


Fig. 6 Selection of MP1 in margin space ( $Mar_2 = 3\%$  and  $Mar_1 = 1\%$ ).

If the margin combination point, MP2 ( $Mar_2 = 1\%$ ,  $Mar_1 = 4\%$ ), is subsequently selected, the iso-contour representing the aircraft range constraint shifts in the other contour plots of the MS, as shown in Fig. 7.

It can be seen from Fig. 7 that the selection of MP2 results in a larger feasible margin space in plot  $Mar_1$  vs.  $Mar_3$ . However, the opposite trend is noticeable in the bottom-right plot ( $Mar_2$  vs.  $Mar_3$ ).

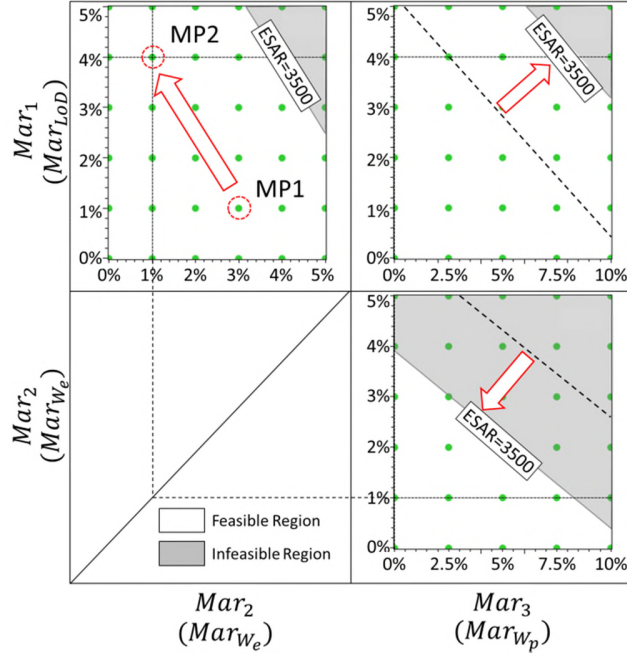


Fig. 7 Selection of MP2 in margin space ( $Mar_2 = 1\%$  and  $Mar_1 = 4\%$ )

By selecting different margin combinations in this manner, the designer can interactively visualize how the feasible margin space changes. Note that, for the simple example in Fig. 6 and Fig. 7, the values for  $Mar_1$  and  $Mar_2$  ( $Mar_{LOD}$  and  $Mar_{We}$ ) were selected first, after which the effects on  $Mar_3$  ( $Mar_{Wp}$ ) was observed. However, the sequence of assigning combinations of margins is up to the designer to choose and can be dependent on the problem under consideration.

### 3.2.1.2. Deterministic design band filtering

In the case where the interest is more on ensuring that minimum values are assigned to the margins, rather than investigating the exact relationships between the margins (and design variables), it is proposed that a parallel coordinates plot (PCP) be utilized. It can be used to filter out solutions that are not capable of providing the minimum requested margin values, subject to performance constraints. The remaining solutions constitute a deterministic design band (DB) in the parallel coordinates plot, which can be represented by:

$$DB = \{(X, M, Y) | G_i(X, M) - g_i \leq 0, i = 1, 2, \dots, p\} \quad (14)$$

The deterministic DB for SIMPCODE is shown in Fig. 8. It is confined by the dashed blue lines. In addition to the design variables ( $AR$  and  $W_f$ ) and performance parameters ( $TOFL$  and  $ESAR$ ), the plot in Fig. 8 also includes the margin parameters ( $Mar_{LOD}$ ,  $Mar_{We}$ , and  $Mar_{Wp}$ ). Here, two criteria are used for filtering out undesirable points: 1) deterministic constraints ( $ESAR \geq 3500nm$ ) and 2) minimum margin requirements (1%, 1% and 2.5%, for margins  $Mar_{LOD}$ ,  $Mar_{We}$ , and  $Mar_{Wp}$ , respectively). The grey



solutions are discarded due to the violation of the deterministic constraint, whereas the yellow solutions are filtered out due to the required minimum margin values not being met.

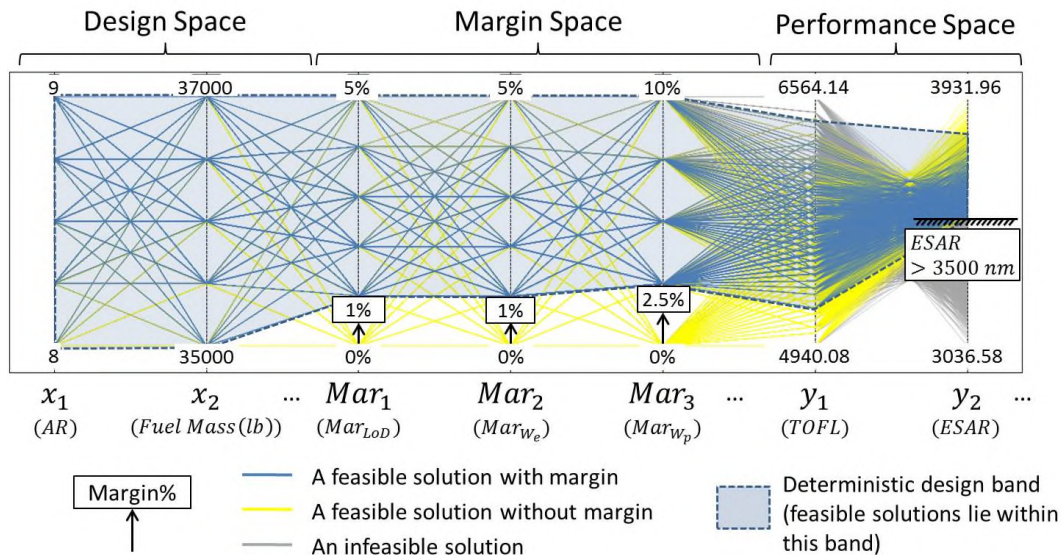


Fig. 8 Deterministic design band (DB) filtering using parallel coordinates plots.

The seamless integration of PCP and contour plots is an effective means for interactive design space exploration and margins trade-off. For example, it may turn out that it is impossible to achieve the desired minimum values for all the margins under consideration, due to not being able to meet the constraints. In such a case, the PCP could be used to find an appropriate combination of minimum margin values by interactively varying the minimum values of the individual margins. Moreover, given that the PCP and the contour plots are interlinked, the designer can simultaneously investigate the positions of the points in their corresponding design and margin spaces and visualize the topology of the feasible regions (e.g., the white regions in, Fig. 5).

### 3.2.2. Trade-off between margins and probability of constraint satisfaction

To initiate this type of trade-off study, information on the probability density functions (PDF) of the uncertain sources must be available. The sources of uncertainty considered in the SIMPCODE example include model uncertainty in the aerodynamic and empty mass models, respectively. To render the outputs ( $LoD$ ,  $W_e$ ) of these models stochastic, a randomization treatment needed to be applied. In this case, the randomization treatment provided in Ref. [19] was employed and the PDFs were assumed to be triangular. It should be noted that, to avoid double accounting of the uncertainty, margins  $Mar_{LoD}$  and  $Mar_{W_e}$  should be removed. The study involves uncertainty propagation and the calculation of the probability of constraint satisfaction for each design point in the design/margin space. Given the large number of design points involved in practice, an efficient approximation method such as the Univariate Reduced Quadrature (URQ) [20] could be chosen for uncertainty propagation. Two techniques are proposed below for trading margins and probability of constraint satisfaction.

### 3.2.2.1. Margin and probability of constraint satisfaction investigation

This technique enables the designer to visually compare different margin combinations with the probabilities of constraint satisfaction. It uses two-dimensional contour plots of the design space, in which iso-contours corresponding to both the margin combinations and probability of constraint satisfaction are shown simultaneously.

Recall from the margin vs. margin trade-offs, discussed in the previous section, that selecting different values of margins will affect the projection of the constraints in the design space (i.e. it will lead to a change of the feasible region, as shown in Fig. 5). Therefore, each margin combination will have a corresponding iso-contour in the design space. Similarly, following uncertainty quantification, the probability of constraint satisfaction for each design point could also be plotted as an iso-contour in the design space. Here, these two iso-contours are combined in a single plot, wherein the designer can interactively change the values of different margins and alter the thresholds for the probabilities of constraint satisfaction.

Employing SIMPCODE again, the technique is illustrated in Fig. 9. The white areas in the 2D design space in the plot in Fig. 9a represent the robust region, where the corresponding probability of constraint satisfaction on *ESAR* is higher than 85%. The iso-contour line represents the location of 85% probability of constraint satisfaction. The iso-contours of different possible margins combinations are shown in Fig. 9b. For this example, an arbitrary margin combination selection is shown in Table 2. The contour line formed by a margin combination, and the associated reduction in the feasible design space can visually be overlapped on the robust/non-robust areas. This is shown in Fig. 9c-d for the different margin combinations in Table 2. The light-red lines represent the iso-contours formed by the margin combination, whereas the light-red shaded areas represent how the feasible design space changes according to the specific combination applied. It can be seen from the plots in Fig. 9c-d, that margin-combination  $C_1$  will fail to meet the required 85% probability of constraint satisfaction, whereas  $C_2$  is sufficient to maintain it, since it is located comfortably inside the robust region.

**Table 2 Trade-off between margins combinations.**

<b>Combination</b>	$Mar_{LoD}$	$Mar_{We}$
$C_1$	3%	2%
$C_2$	1%	5%

In addition, by visually comparing the intersection angles of the two types of iso-contours, the designer could deduce whether the margins are allocated appropriately. For instance, a  $90^\circ$  angle between a constraint (iso-contour corresponding to a particular margin combination) and a probability iso-contour would indicate that they are not correlated (i.e. low sensitivity with respect to each other). In other words, altering the margin will not change the probability of constraint satisfaction of the design points that remain in the robust region. This, in turn, implies that the margins in question can be reallocated elsewhere.

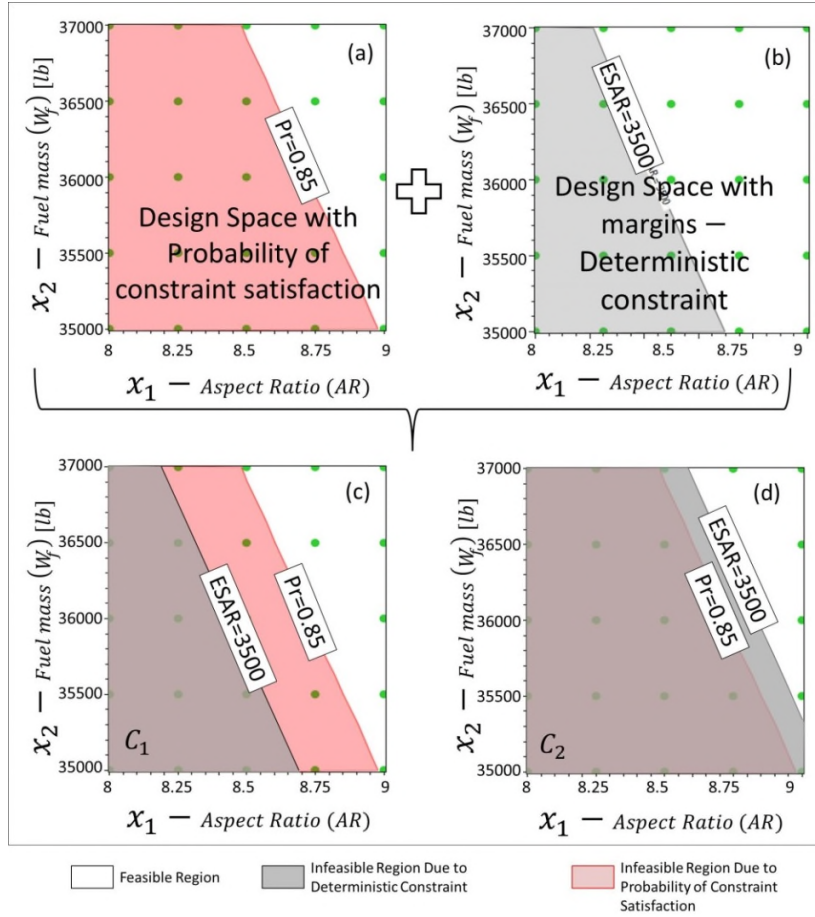


Fig. 9 Probability of constraint satisfaction vs. margin combinations.

### 3.2.2.2. Robust design band filtering

Filtering can be used to discard design solutions with certain margin combinations that do not meet the required probability of constraint satisfaction. In this case, the parallel coordinates plot can be used to first filter out infeasible designs and then to find the minimum margin values according to specified probability satisfaction thresholds. The result of doing this is a robust design band ( $DB^r$ ), which can be represented by:

$$DB^r = \{(\mathbf{X}, \mathbf{M}, \mathbf{Y}) | P_i(G_i(\mathbf{X}, \mathbf{M}) - g_i \leq 0) \geq P_i^t, i = 1, 2, 3, \dots, p\} \quad (15)$$

Consider SIMPCODE, with the threshold on probability of satisfying the  $ESAR$  ( $Pr_{ESAR}$ ) constraint, set as 85%. Design solutions that fail to meet this threshold are shown by the red lines in Fig. 10. These can be discarded. (Note that this type of filtering also results in a reduction of the number of polylines in the deterministic  $DB$  defined in Section III-B). The resulting robust design band is shown in Fig. 10 as the region enclosed by the dashed blue lines.

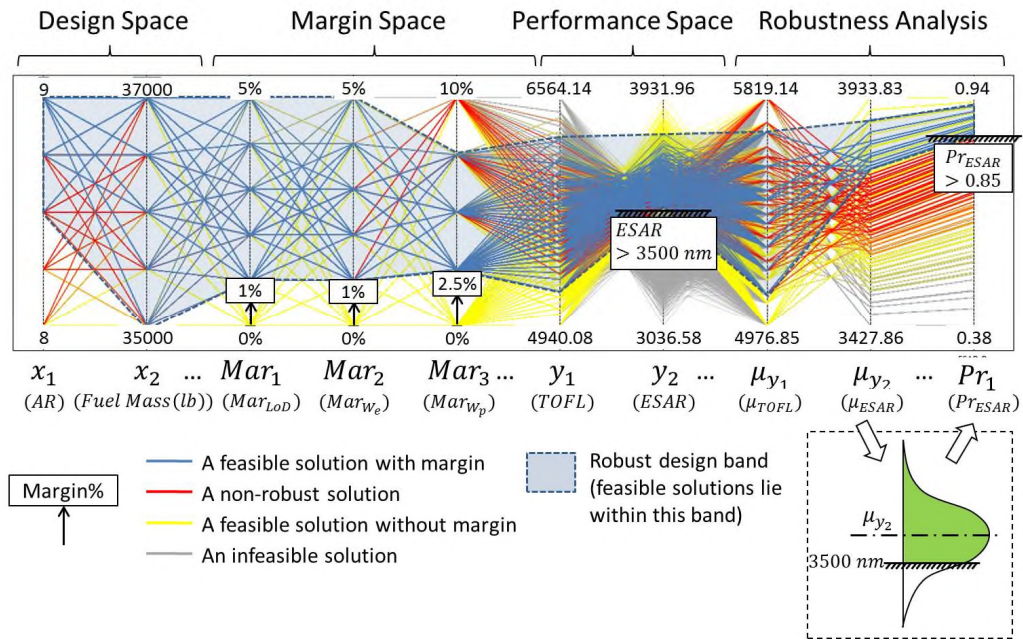


Fig. 10 Robust design band ( $DB^*$ ) filtering using parallel coordinates plots.

### 3.2.3. Trade-offs between margins and performance

In general, the allocation of margins adversely affects performance, as it involves placing ‘reserves’. The purpose of trading-off margins with performance parameters is therefore to identify combinations of margins that adequately account for uncertainty, but still allow acceptable performance. A technique using scatter plots is presented for interactively exploring the change in the location of the Pareto front when the margin values are varied.

In this technique, a two-dimensional scatter plot is used to investigate the effect of the selected margin combinations in the performance space. Using SIMPCODE again, Fig. 11 shows a two-dimensional scatter plot of the performance space where smaller values for  $TOFL$  and larger values for  $ESAR$  are sought. The Pareto front in Fig. 11, comprised by the non-dominated solutions, is depicted by the black dashed line and corresponds to the zero-margin values combination,  $C_0$ .

The other two dashed lines (green and purple) represent the Pareto fronts corresponding to two different combinations of nonzero margin combinations  $C_1$  and  $C_2$ , respectively. As can be seen from Fig. 11, margin combination  $C_1$  provides better performance compared to margin combination  $C_2$ . The designer can therefore use this technique to vary the values of the margins interactively and simultaneously observe the resulting movement of the Pareto front towards degradation or improvement of performance.

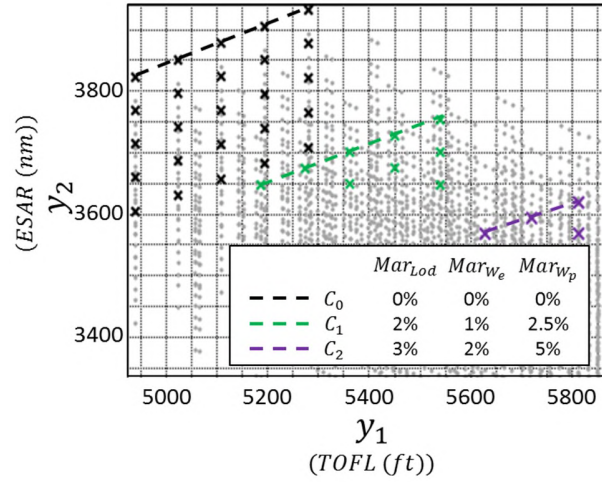
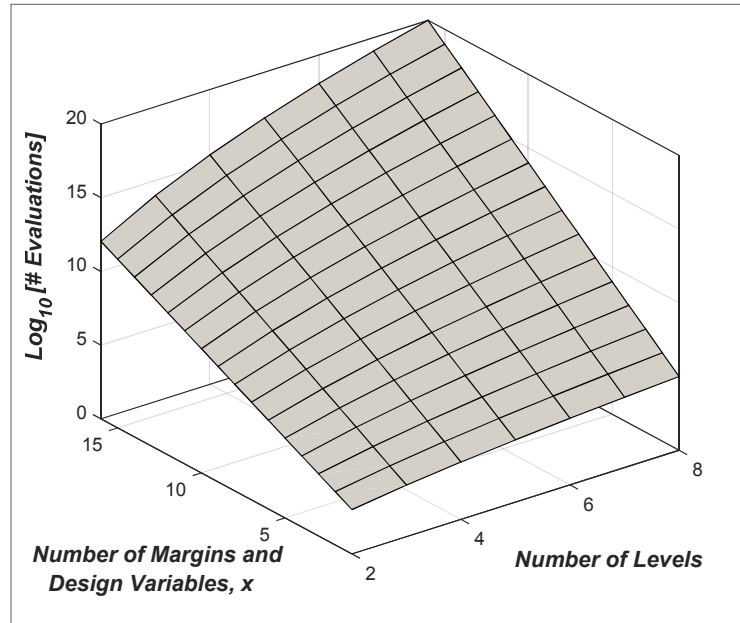


Fig. 11 Effect of different margin combinations on the location of the Pareto front.

### 3.3. Computational effort

Despite the intended use of the proposed framework at early design stages with the employment of low order (fast) models, computational effort is still an important factor. In its current implementation, the computational cost of the framework is due mainly to the full factorial sampling (FFS) used by the constraint analysis method [10].

The FFS computational cost is exponential ( $O(l^x)$ , where  $x = r + n$  is the total number of design variables and margins and,  $l$  is the number of levels. Fig. 12 illustrates the upper bound of the number of evaluations for different values of  $x$  and  $l$ , required by FFS. It is an upper bound, because, in this case, the same number of levels applies to all design and margin variables. The plot shows that the sampling approach becomes impractical for high dimensional problems.



**Fig. 12 Sampling computational cost**

The computational cost and ways of reducing it are discussed in more detail in Section IV-E.

## 4. Evaluation

A qualitative evaluation and validation of the proposed framework was undertaken as part of the TOICA (Thermal Overall Integrated Conception of Aircraft) research project [1]. As mentioned in the introduction, the overall requirements for an extended margin management system were extracted during the initial stages of the project through a requirements elicitation process involving experienced aircraft and airframe systems architects [2]. The validation involved determining whether the framework presented herein met the following user requirements:

- Explicitly specify the margins;
- Work simultaneously with margin and design (spaces), and
- Perform interactive trade-offs.

To perform the evaluation, the methods and enablers proposed in Section III were implemented into an existing in-house model-based design tool, called AirCADia [21]. This software tool contains inbuilt enablers for performing optimization, design space exploration, as well as deterministic and robust design studies. The proposed framework and the prototype tool were demonstrated at the TOICA project milestones through an industrially relevant test case. The feedback from the practicing experienced



designers and airframe systems architects confirmed the potential usability of the framework in an industrial context. One area identified for improvement was the definition of an *explicit* margin policy (at the time this was handled implicitly through the parallel coordinates plots). This deficiency was addressed by introducing the explicit margin space concept, as described in Section III-A.

The rest of this section presents a summary of the evaluation test case.

#### 4.1. Test case description

A conceptual sizing study involving a short-range passenger aircraft was considered. A simplified high-level view of the computational workflow of this study is shown in Fig. 13 and nomenclature in Table 3. The margins applied are shown in blue rectangles. For the sake of simplicity, only nine out of the 28 variables on which margins were applied are shown in the figure.

Table 3 Test case nomenclature.

Category	Symbol	Name
Aircraft Level	$DesRng$	Design Range [nm]
	$S_w$	Wing Reference Area [ $ft^2$ ]
	$SLST$	Engine Sea-Level Static Thrust [lbf]
	$GW$	Gross Weight [lb]
	$V_{app}$	Approach Velocity [kt]
	$TOFL$	Take-Off Field Length [ft]
	$LFL$	Landing Field Length [ft]
	$NO_x$	Nitrogen Oxide Emissions [lb]
	$SLNoise$	Sideline Noise [EPNdB]
	$FONoise$	Flyover Noise [EPNdB]
	$BlockFuel$	Block Fuel [lb]
	$FASM$	Fuel per Available Seat Mile [lb/nm]
	$SP_{OT}$	Total Shaft Power Off-Take [kW]
	$M_{sys}$	Total System Mass [lb]
$N_{pax}$	Number of Passengers	
Environment Control System (ECS)	$\dot{m}_{PerOcpmin}$	Mass Flow Rate of Fresh Air per Occupant [kg/s]
	$T_{inmin}$	Temperature of Air Flow into the Cabin [°C]
	$c_{wall}$	Fuselage skin heat transfer coefficient [W/(m <sup>2</sup> K)]
	$\dot{Q}_{FD}$	Heat load from the flight deck [W]
	$M_{ECS}$	ECS Mass [lb]
	$P_{ECS}$	ECS Power Off-Take [kW]
	$Mar_{\dot{m}_{PerOcp}}$	Margin on Mass Flow Rate of Fresh Air per Occupant
	$Mar_{T_{inmin}}$	Margin on Temperature of Air Flow into the Cabin
	$Mar_{M_{ECS}}$	Margin on ECS Mass
Flight Control System (FCS)	$S_{HT}$	Horizontal Tail Reference Area [ $ft^2$ ]
	$S_{VT}$	Vertical Tail Reference Area [ $ft^2$ ]
	$M_{FCS}$	FCS Mass [lb]
	$P_{FCS}$	FCS Power Off-Take [kW]
	$Mar_{M_{FCS}}$	Margin on FCS Mass

	$Mar_{P_{FCS}}$	Margin on FCS Power Off-Take
Ice Protection System (IPS)	$T_{skin}$	Required Skin Temperature [K]
	$S_{PROTW}$	Total Protected Area for Wing IPS [ $m^2$ ]
	$S_{PROTNAC}$	Total Protected Area for Cowling IPS [ $m^2$ ]
	$M_{IPS}$	IPS Mass [lb]
	$P_{IPS}$	IPS Power Off-Take [kW]
	$Mar_{T_{skin}}$	Margin on Required Skin Temperature
	$Mar_{M_{IPS}}$	Margin on IPS Mass
	$Mar_{P_{IPSW}}$	Margin on Wing IPS Power Off-Take
	$Mar_{P_{IPSC}}$	Margin on Cowling IPS Power Off-Take

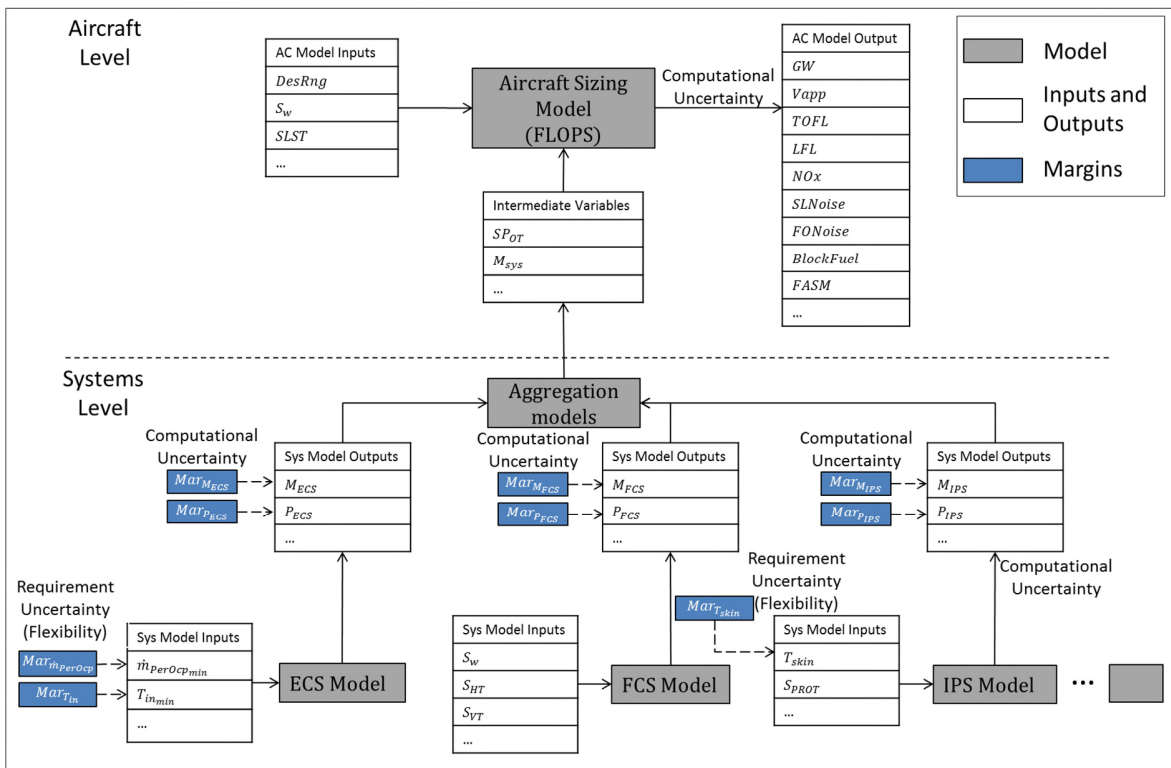


Fig. 13 Schematic computational workflow of the design study.

The workflow is divided into two hierarchical levels: overall (top) aircraft level and subsystems level. The top level contains the computational models for aircraft geometry and performance, whereas the models at the subsystem level compute subsystem attributes and performance, such as weight and power offtake. The data employed are realistic, but do not represent an actual aircraft, since the purpose was solely to demonstrate the capabilities and benefits of the proposed framework.

At aircraft level, the NASA Flight Optimization System (FLOPS) [22] was used for aircraft sizing and performance analysis. Models for the subsystems were assembled from several research papers [23]–[27]. The outputs of the system models were aggregated and linked to the aircraft level to compute the total



engine shaft power offtake and systems weight. All models were assembled into a computational workflow using the dynamic (automatic) workflow creation module [6] in AirCADia. In total, 171 models and 317 variables comprise the workflow.

## 4.2. Initial margin allocation

After the set-up of the computational workflow, margins were allocated (on 28 variables with values of up to 30%) to address two types of uncertainty: uncertainty in the requirements and uncertainty in the computational models. For example, as shown in Fig. 13,  $Mar_{\dot{m}_{PerOcp}}$  was applied to account for changes in the fresh air mass flow rate requirement on the environmental control system (ECS), whereas  $Mar_{M_{ECS}}$  was applied to account for uncertainty in the output of the computational models calculating the mass of the ECS.

In order to determine which of the 28 margins would be the most influential, a sensitivity analysis was performed, using the Fourier-Amplified Sensitivity Test (FAST) [28]. Without loss of generality, uniform distributions, ranging between 0 and 30%, were used for all the margin values.

The five most influential margins turned out to be,  $Mar_{\dot{m}_{PerOcp}}$ ,  $Mar_{M_{ECS}}$ ,  $Mar_{M_{FCS}}$ ,  $Mar_{P_{ECS}}$ , and  $Mar_{M_{EPS}}$ . The first three of these were of particular interest for this study.

A full factorial sampling (FFS) study was then performed in AirCADia to populate the design space with potential solutions. Two design variables, wing reference area ( $S_W$ ) and sea-level static thrust ( $SLST$ ) were considered. The arbitrarily selected bounds of the design variables and the corresponding number of levels for the FFS are listed in Table 4, along with the lower and upper bound values of the three considered margins. The performance constraints considered during the test case demonstration are listed in Table 5.

Table 4 Design of experiments study formulation.

Category	Parameter	Lower bound	Upper bound	Levels
Design Variables	$S_W$ ( $ft^2$ )	1350	1390	5
	$SLST$ ( $lb$ )	27000	29000	5
Margins	$Mar_{m_{PerOcp}}$	0%	30%	4
	$Mar_{M_{ECS}}$	0%	30%	4
	$Mar_{M_{ECS}}$	0%	30%	4

Table 5 Performance constraints.

Parameter	Limiting value
$TOFL$	$\leq 5500$ $ft$
$V_{app}$	$\leq 136$ $kt$
$Nox$	$\leq 500$ $lb$

### 4.3. Margins trade-off

For this demonstration, the trade-off sequence was assumed to be in the following order: 1) margins with margins, 2) margins with probabilities of constraint satisfaction, and 3) margins with performance. However, as stated earlier, the designer may choose any sequence as part of an iterative process.

#### 4.3.1. Margin with margin

Recall from Section III that the allowable ‘room’ for allocating a margin is dependent on the selected design point and the selected magnitudes of the other margins. This can be seen again in Fig. 14, where the design space and corresponding margin spaces for design points A ( $S_W = 1380$   $ft^2$ ,  $SLST = 28000$   $lb$ ) and B ( $S_W = 1380$   $ft^2$ ,  $SLST = 28500$   $lb$ ) are shown, respectively. Both figures represent two-dimensional ‘slices’ of the multidimensional design and margin spaces, with the constraints on take-off field length ( $TOFL$ ), approach velocity ( $V_{app}$ ) and fuel per assigned-seat-mile ( $FASM$ ) represented as iso-contours. It can be observed that design point B would provide more freedom for allocating margins compared with design point A, as indicated by the white feasible regions in the 2D plots.

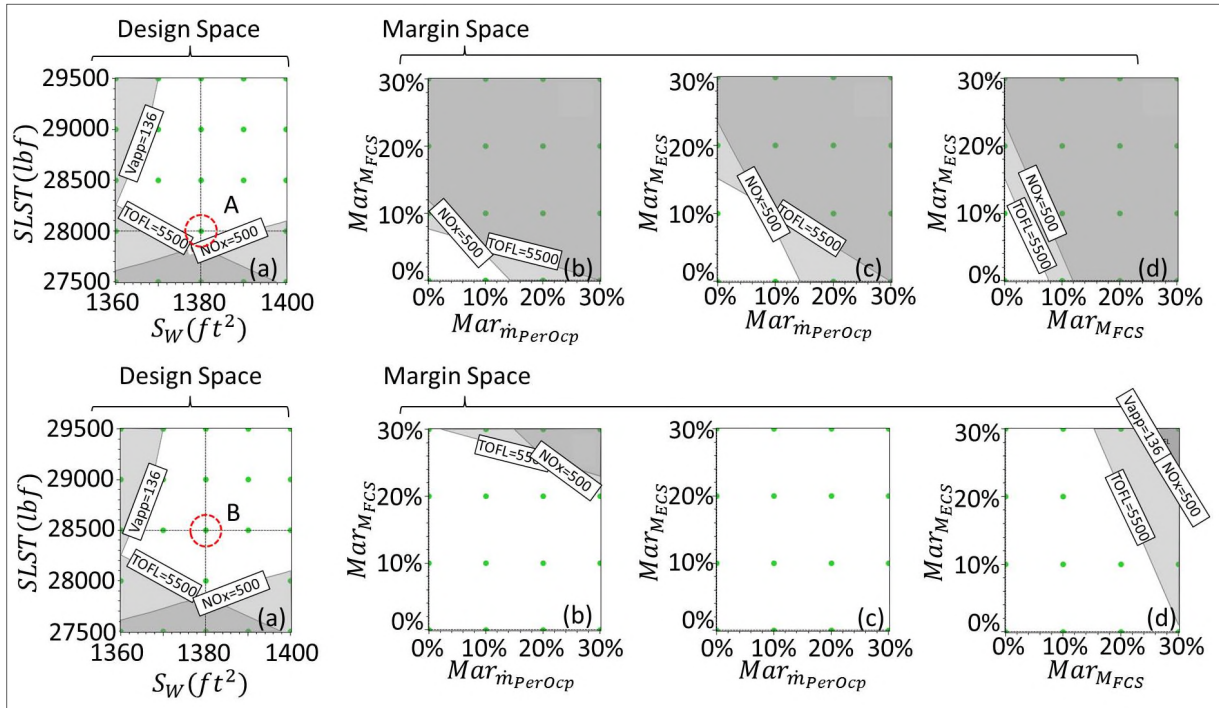


Fig. 14 Margin exploration for designs A and B.

After selecting a design point and assigning initial, margin values, the designer can undertake to trade these off. Since (as described in Section III) assigning a value for a particular margin affects the allowable values for the other margins, the user must choose a sequence for assigning the values. Assume design point B is chosen in the design space and a decision was made to allocate a 20% margin on FCS mass ( $Mar_{M_{FCS}} = 20\%$ ) and 10% margin on the ECS fresh air mass flow rate ( $Mar_{\dot{m}_{PerOcp}} = 10\%$ ). This is shown in Fig. 15. Doing so results in an allowable room for margins on the ECS masses ( $Mar_{M_{ECS}}$ ), which may not be sufficiently large. Subsequently, selecting a different point in the margin space (MS), i.e. 10% margin on FCS mass and 20% margin on the ECS fresh air mass flow rate will modify the feasible (allowable) margin space, as shown in Fig. 16.

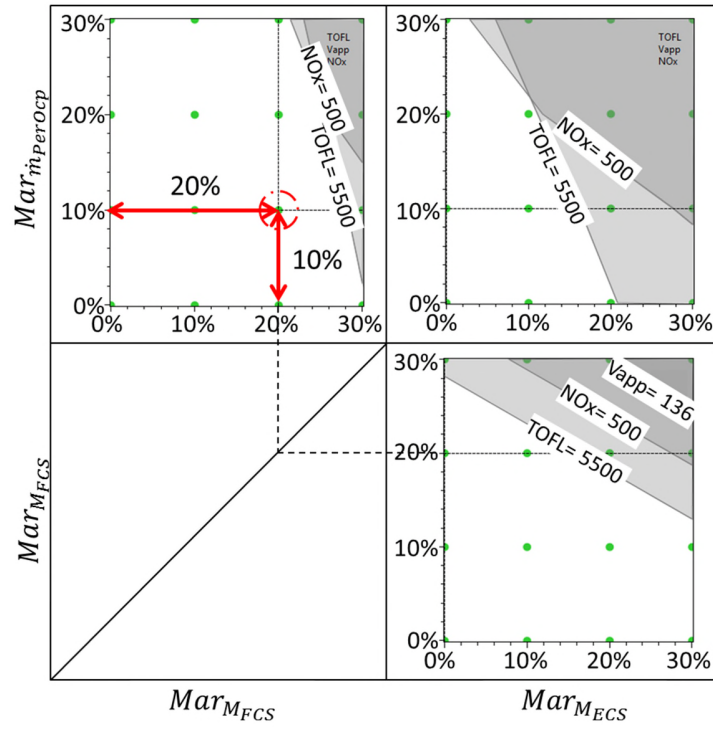


Fig. 15 Feasible margin space for point B when  $Mar_{MFCS} = 20\%$  and  $Mar_{\dot{m}_{perOcp}} = 10\%$ .

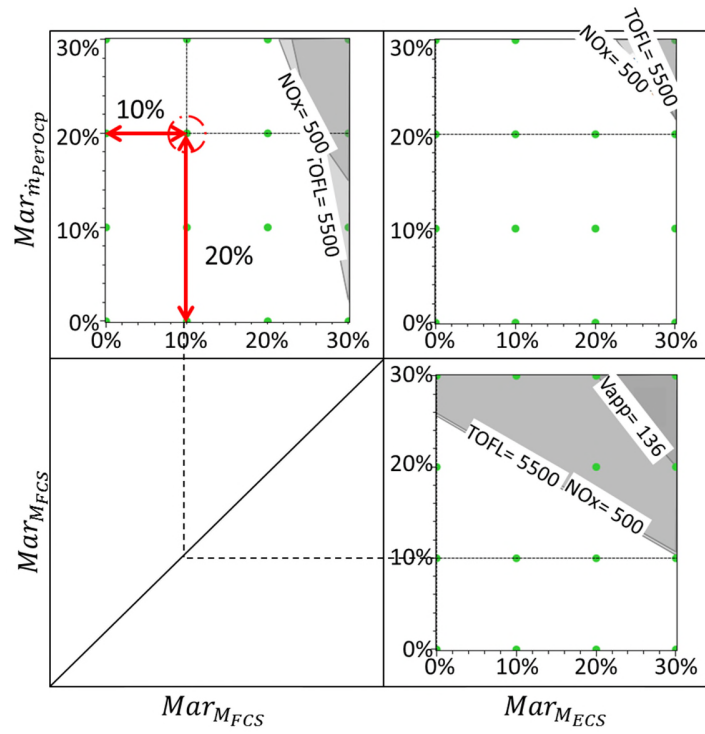


Fig. 16 Feasible margin space for point B when  $Mar_{MFCS} = 10\%$  and  $Mar_{\dot{m}_{perOcp}} = 20\%$ .

Finally, suppose a decision was made to secure a value of at least 10% for all the margins. This would reduce the feasible design space to that shown in Fig. 17 with a subsequent reduction in the number of design points with different margin combinations from 1600 to 124. The parallel coordinates plot in Fig. 17 shows the deterministic design band, which is represented by the region enclosed by the dashed-blue lines. All the design points in this band could therefore be allocated margins of at least 10% on ECS mass, FCS mass, and ECS mass flow rate, and remain feasible. It is important to note that, after selecting the minimum value of 10% on all the chosen margins, the allowable room for margin on the  $TOFL$  requirement reduces to only 0.6%. This value is calculated by comparing the current constraint ( $TOFL \leq 5500 \text{ ft}$ ) and the take-off field length calculated at the selected desirable point in the design/margin space (in this case,  $TOFL' = 5467 \text{ ft}$ ). It should be noted that the green double headed arrow in Fig. 17 (b) is not a margin, but the distance between the current performance constraint and the best achievable one through trade-off (indicated by the green dash line).

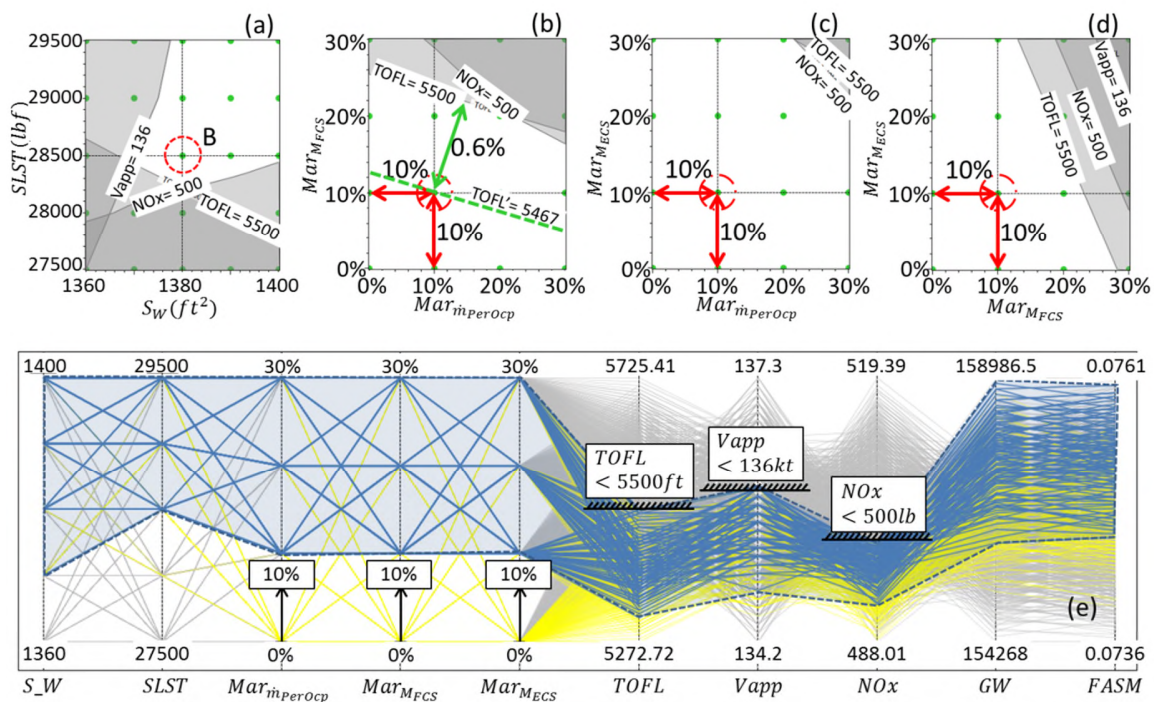


Fig. 17 Deterministic design and margin space.

#### 4.3.2. Trade-off margins with probability of constraint satisfaction

After reducing the feasible design/margin space, a robustness analysis was conducted. The purpose was to find margin magnitudes that are large enough to maintain design robustness. The sources of uncertainty considered, along with the assumed distributions, are listed in Table 6. These include both input and model uncertainties. Generally, such distributions can be obtained from historical data and/or expert elicitation.

Table 6 Sources of uncertainty.

Simulation parameter	Corresponding random variable	Distribution
$c_{wall}$	$R_{c_{wall}}$	Uniform distribution: lower bound=1; upper bound=1.4
$\dot{Q}_{FD}$	$R_{\dot{Q}_{FD}}$	Uniform distribution: lower bound=0.8; upper bound=1.2
$M_{ECS}$	$R_{M_{ECS}}$	Triangular distribution: lower bound =0.7; mode=1; upper bound =1.3
$M_{FCS}$	$R_{M_{FCS}}$	Triangular distribution: lower bound =0.7; mode=1; upper bound =1.3

The earlier mentioned URQ technique [20], was employed to propagate the uncertainty for each design point. However, prior to doing this, the margins on ECS and FCS mass had to be removed, since placing uncertainty distribution on the parameter value in addition to its margin would result in double accounting for uncertainty. This was not required for the margins on  $Mar_{\dot{m}_{perOcp}}$  and  $Mar_{DesRng}$ , since these were applied to accommodate flexible requirements, whereas the margins on ECS mass and FCS mass were specifically applied to accommodate uncertainty (lack of confidence) in the computational model.

The user could interactively adjust the margins and probability thresholds to perform trade-off studies, as shown in Fig. 18 for margin combinations listed in Table 7. Assume that the required probabilities of constraint satisfaction for  $TOFL$ ,  $V_{app}$ , and  $NOx$  were all selected to be 90%. This defines the robust (white) and non-robust (grey shaded) regions in the design space, as indicated in Fig. 18a.

Note that the lines representing the 90% probability of constraint satisfaction are ‘jagged’. This is because of the non-linear nature of the Gaussian, projected onto the design space. If higher-order interpolation is used, the lines will be smoother, but still not straight. In addition, as explained at the beginning of Section IV-C-2, the probability of constraint satisfaction can be a function of the selected margins. In this case, the probability of constraint satisfaction is a function of  $Mar_{\dot{m}_{perOcp}}$ , and it can be seen in Fig. 18 that the location of the iso-contours corresponding to 90% probability of constraint satisfaction changes for different values of this margin.

Following the approach described in Section III-B-2 the contours formed in the design space, resulting from the allocation of deterministic margins, can now be combined (overlapped) with the probabilistic region. This is illustrated in Fig. 18a-d, where the blue lines represent the deterministic contours and the blue-shaded regions represent the infeasible regions for particular margin combinations (Table 7). Note that these margin combinations are different from the SIMPCODE example. As can be seen in the figure, combinations that are more stringent constrict the design space further. A reasonable selection would be  $C_2$  which would ‘just’ cover the probabilistic constraints (i.e. rendering the design space slightly smaller than what it would have been with only the probabilistic constraints present). An undesirable case will be the margin combination  $C_4$ , where the  $NOx$  constraint renders the design space infeasible.

Table 7 Selection of possible margin combinations for trade-off with probability of constraint satisfaction.

Combination	$Mar_{M_{ECS}}$	$Mar_{M_{FCS}}$	$Mar_{m_{PerOcp}}$
$C_1$	10%	10%	10%
$C_2$	10%	20%	20%
$C_3$	30%	30%	20%
$C_4$	30%	30%	30%

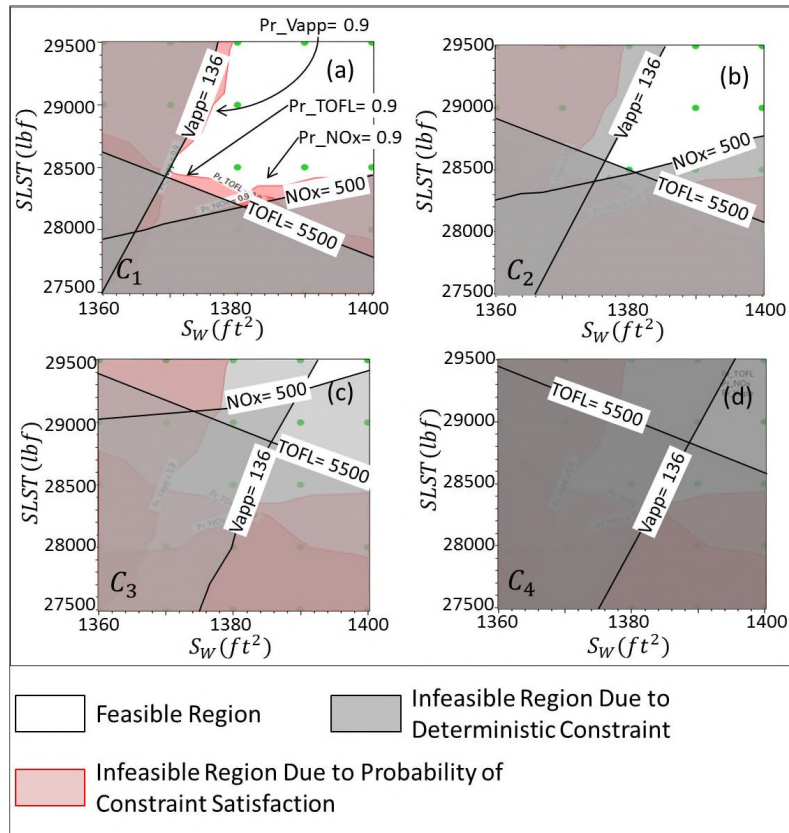


Fig. 18 Combinations of margins with 90% probability constraint satisfaction for all constraints.

To determine the RDB, 90% thresholds were placed on the probabilistic constraints. (PCP not shown here for brevity). In this case, only three points were discarded, which means that the 10% values assigned to the margins (in Fig. 17) were sufficient to account for uncertainty.

#### 4.3.3. Trade-off margins with performance

As described in Section III, a Pareto front investigation can be applied to understand the effect of the selected margin combinations on the performance space. Recall that assigning different combinations of margins lead to ‘shifting’ of the Pareto front corresponding to the selected margin combination in the



performance space. A similar situation is illustrated here in Fig. 19 for different margin combinations. The performance parameters considered are the nitrogen oxide emissions ( $NOx$ ) and fuel per available seat mile ( $FAM$ ). Combination  $C_1$  (represented by the red dashed line) provides the best performance compared to the other margin combinations.

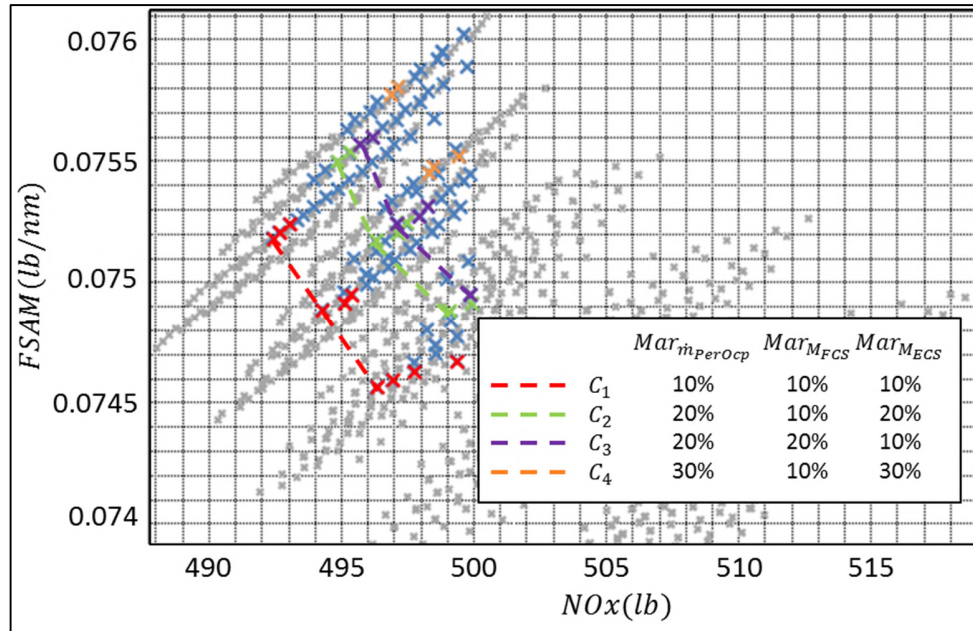


Fig. 19 Effect of combinations of margins on the location of the Pareto front.

A parallel coordinates plot can be used to further down-select the design points. For instance, if the designer identifies that  $C_3$  (represented by the purple dashed line in Fig. 19) is the margin combination that better compromises performance versus robustness, then he/she can use the parallel coordinates plot to filter out the margin value combinations above  $C_3$ . This results in the reduction of the number of design points from 121 down to 30.

#### 4.4. What-if scenarios

The trade-off techniques presented in the previous section enable the designer to investigate two types of what-if scenarios:

- If the weight growth for a certain system exceeds the assigned margin, then the designer can reduce margins from other systems, if possible, and allocate it to the system with exceeded weight. For example, if at a stage of the design process it is found that the selected margin on the mass of the FCS,  $Mar_{M_{FCS}}$ , is not sufficient, then he/she can attempt to reduce the margin on the mass allocated to the ECS,  $Mar_{M_{ECS}}$ , and assign extra margin on the mass of the FCS. Fig. 20 illustrates such a case, where the initial margin combination is shown by the red arrows and a possible, revised selection by the blue arrows.



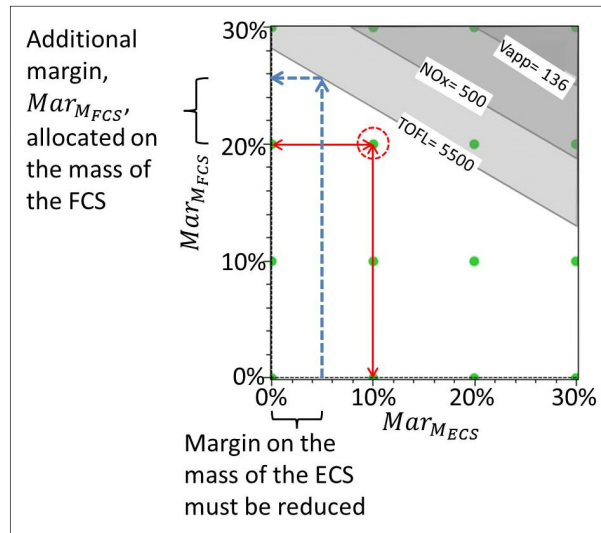


Fig. 20 Reallocation of margins from one system to another.

- If, for whatever reason, a requirement changes (for example, a reduction in take-off field length,  $TOFL$ ), the designer can proceed with one of the following two options:
  - Trade between different margins (as described above) and/or reduce margin values. Reducing margin values may or may not have significant effect on performance, i.e., it may not be able to satisfy the new requirements. As shown in Fig. 21a, the selected point in the margin space allows a scope for only 0.6% reduction in the  $TOFL$  constraint value. (Note that the meaning of the green arrows is the same as explained earlier with regard to Fig. 17). This scope could be increased to 1% if the margins  $Mar_{M_{FCS}}$  and  $Mar_{M_{\dot{m}_{PerOcp}}}$  are relaxed, as shown in Fig. 21b. However, if the required increase in the  $TOFL$  requirement is 5%, no applied margin combination is feasible, as shown in Fig. 21c.

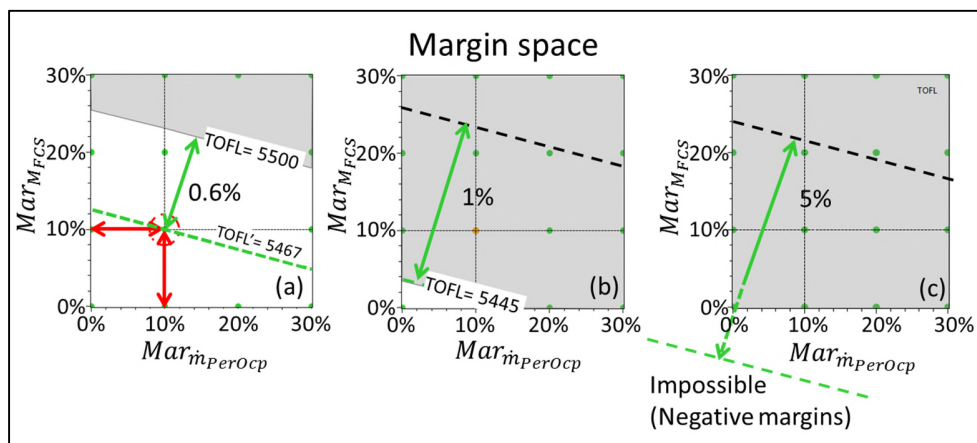


Fig. 21 Accommodating change of take-off field length  $TOFL$  requirement.

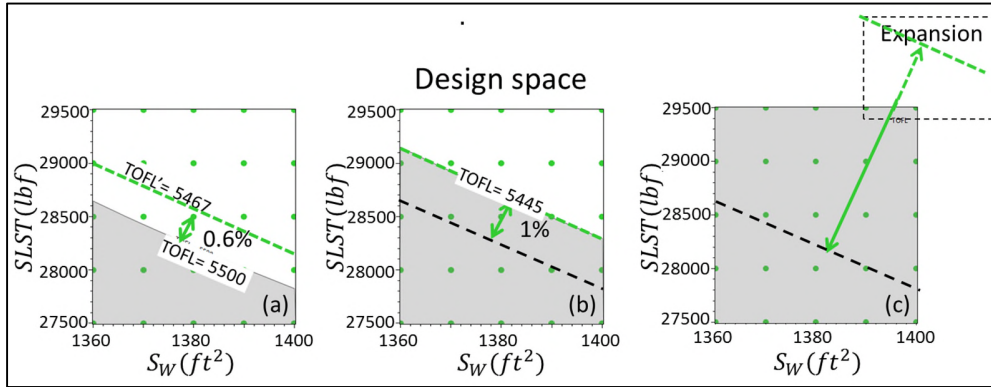


Fig. 22 Required extension of the design space to accommodate the desired margin.

- An investigation in the design space shows that, even when changing to another design point, the margin of 5% can still not be achieved by any design and margin combination. A possible course of action is that the design space can be extended utilizing the knowledge gained during the design and margin space exploration. Not surprisingly, in this case study, the harder *TOFL* constraint can be met by increasing the wing area and/or sea-level static thrust, as shown by the direction of the red arrow in Fig. 22b and c.

#### 4.5. Computational cost

With reference to Table 4, the computational effort in this case requires 1600 evaluations, considering the sampling of both the design and margin spaces. The generation of data for the entire test case took approximately three minutes on a standard PC, using one Intel i7-2600 processor with a 3.6GHz CPU. The sensitivity analysis of the 28 candidate margins required 19209 model evaluations and took approximately 1 hour 20 minutes on the same PC. The alternative would have been to sample a margin space of 28 variables, which would have been prohibitively expensive, as indicated in Section III-C.

Considering the importance of computational cost, the following avenues for its reduction could be pursued:

- When performing a FFS, a reasonable choice of the levels,  $l$ , can be made. For example, assuming,  $x=8$ , and each model evaluation taking 0.25s, a reasonable choice of levels could be  $l=5$ . In such a case the study will require 390625 evaluations (approximately 27 hours). This is acceptable for an ‘over the weekend job’.
- Moreover, alternative methods, designed specifically to increase sampling efficiency have been proposed in the literature (e.g. Latin Hypercube [9], Sobol’ sequence [29], etc.) and their practical investigation forms part of future work.
- As mentioned above, given a large number ( $x$ ) of design variables and margins, a practical solution would be to conduct a sensitivity analysis study in order to select a few most influential design or margin variables. In this work, the Fourier-Amplified Sensitivity Test (FAST) method [28] is employed because of its maturity and since its computational cost approximates quadratic time complexity. Other, even faster methods [30] could be employed to that purpose.

- Finally, the nature of the demanding computations (e.g., sampling/DoE) described here are amenable to parallelization and thus to the employment of high performance computing. This is beyond the scope of the current work, but can be a viable option in industry.

## 5. Conclusions

Presented is an interactive approach for margins allocation and trade-off, in the context of model-based design of complex systems. Central to this approach is the introduction of the concept of explicit ‘margin space’ (*MS*). An *MS* is derived from, and bi-directionally linked to the design space. By contrast to existing practice, based largely on subjective experience, this approach enables a designer to explore and understand how assigning margins on certain parameters affects the allowable margins that can be assigned to other parameters. The overall approach is facilitated by a framework, which integrates methods for efficient uncertainty propagation, input-output reversal of computational workflows and design exploration means such as design space sampling techniques, interactive iso-contours, and parallel coordinate plots. Specifically, these allow decision makers, such as designers and product architects, to conduct interactive trade-offs between margins and margins, margins and performance, and margins and uncertainty (probability of constraint satisfaction). This was made possible by rendering the relationship between design variables, margins, and performance variables explicit, as well as through the design exploration means described above.

The approach and the associated enablers were implemented into a prototype software tool, AirCADia, which was used for a qualitative evaluation by practicing designers. The evaluation, conducted as part of the EU TOICA project, confirmed the practicality of the approach. In particular, the explicit specification of margins, relationship between design variables, margins, and performance variables, and bi-directional links between margins and design spaces, demonstrated that the requirements prescribed by the industrial stake-holders were largely met.

Future work will focus on advancing the proposed framework to enable more complex and distributed computations, involving fast, component-based sizing of airframe systems. Aspects that require further investigation include:

- The generalization of the method to encompass margin trade-offs between different product decomposition levels, accounting for ‘transversal’ effects, such as heat emissions. This, in turn, will require taking into account the geometry and spatial layout at appropriate (parsimonious) levels of detail.
- An extension of the approach to deal with potentially correlated inputs and also possible double accounting of margins, e.g. through coupled (dependent) parameters.
- Developing a method accounting for margin composition along the design process. That is, as knowledge increases, the proportion of the margin due to uncertainty (e.g. lack of maturity) should ideally diminish, while the proportion accounting for design flexibility should not decrease.
- Developing the iso-contour method further to handle sparsity of the sampling (affecting the position of the contour lines), discontinuity of the model and reduction of the computational cost. This will require investigating sampling strategies more efficient than the FFS technique, for example, Latin Hypercube [9], Sobol’ sequences [29], and so forth.

## Acknowledgments

The research leading to these results was funded by the European Union Seventh Framework Programme (FP7/20013-2016, TOICA project), under grant agreement n° 604981.

## References

- [1] Arbez, P., “Innovations in Aircraft Architecture Trade-off,” *Seventh European Aeronautics Days: Aviation in Europe – Innovation for Growth*, London: 2015.
- [2] Rouvreau, S., Mangeant, F., and Arbez, P., “TOICA – Innovations in Aircraft Architecture Selection, Uncertainty Management in Collaborative Trade-offs,” *6th IC-EpsMsO - 6th International Conference on Experiments/Process/System Modeling/Simulation/Optimization*, Athens, Greece: 2015.
- [3] Kockler, F., Withers, T., Poodiack, J., and Gierman, M., *Systems Engineering Management Guide*, Fort Belvoir, VA: Defense Systems Management Coll (DTIC) Document, 1990.
- [4] Cooke, R. M., Zang, T. A., Mavris, D. N., and Tai, J. C., “Sculpting: A Fast, Interactive Method for Probabilistic Design Space Exploration and Margin Allocation,” *16th AIAA/ISSMO Multidisciplinary Analysis and Optimization Conference*, American Institute of Aeronautics and Astronautics, 2015.
- [5] Zang, T. A., Mahadevan, S., Tai, J. C., and Mavris, D. N., “A Strategy for Probabilistic Margin Allocation in Aircraft Conceptual Design,” *16th AIAA/ISSMO Multidisciplinary Analysis and Optimization Conference*, American Institute of Aeronautics and Astronautics, 2015.
- [6] Guenov, M. D., Fantini, P., Balachandran, L. K., Maginot, J. P., and Padulo, M., “MDO at Pre Design Stage,” *Advances in Collaborative Civil Aeronautical Multidisciplinary Design Optimization*, E. Kessler and M.D. Guenov, eds., Reston, VA: American Institute of Aeronautics and Astronautics, 2010, pp. 83–108.
- [7] Raymer, D. P., *Aircraft Design: A Conceptual Approach*, Reston, VA: American Institute of Aeronautics and Astronautics, 2012.
- [8] Jenkinson, L. R., Simpkin, P., and Rhodes, D., *Civil Jet Aircraft Design*, Butterworth-Heinemann: London., 1999.
- [9] Montgomery, D. C., Myers, R. H., and Anderson-Cook, C. M., *Response Surface Methodology: Process and Product*

*Optimization using Designed Experiments*, New Jersey: Wiley, 2009.

- [10] Riaz, A., "Set-Based Approach to Passenger Aircraft Family Design," PhD thesis, Cranfield University, 2015.
- [11] Inselberg, A., "The Plane with Parallel Coordinates," *The Visual Computer*, vol. 1, 1985, pp. 69–91.
- [12] Nunez, M., Maginot, J., Padulo, M., and Guenov, M., "Integrated Exploration and Visualization of Optimal Aircraft Conceptual Designs," *50th AIAA/ASME/ASCE/AHS/ASC Structures, Structural Dynamics, and Materials Conference*, American Institute of Aeronautics and Astronautics, 2009.
- [13] McManus, H., and Hastings, D., "A Framework for Understanding Uncertainty and its Mitigation and Exploitation in Complex Systems," *15th Annual International Symposium of the INCOSE*, Rochester, NY: Wiley Online Library, 2005, pp. 484–503.
- [14] Thunnissen, D. P., "Method for Determining Margins in Conceptual Design," *Journal of Spacecraft and Rockets*, vol. 41, 2004, pp. 85–92.
- [15] Thunnissen, D. P., and Tsuyuki, G. T., "Margin Determination in the Design and Development of a Thermal Control System," *International Conference On Environmental Systems*, SAE International, 2004.
- [16] Thunnissen, D. P., "Propagating and Mitigating Uncertainty in the Design of Complex Multidisciplinary Systems," PhD thesis, California Institute of Technology, 2005.
- [17] Helton, J. C., *Conceptual and Computational Basis for the Quantification of Margins and Uncertainty*, Sandia National Laboratories (United States). Funding organisation: US Department of Energy (United States), 2009.
- [18] O'Connor, P., and Kleyner, A., *Practical Reliability Engineering*, Chichester: John Wiley & Sons, 2012.
- [19] Molina-Cristóbal, A., Nunez, M., Guenov, M. D., Laudan, T., and Druot, T., "Black-box Model Epistemic Uncertainty at Early Design Stage. An Aircraft Power-Plant Integration Case Study," *29th Congress of the International Council of the Aeronautical Sciences, ICAS 2014*, 2014.
- [20] Padulo, M., Campobasso, M. S., and Guenov, M. D., "Novel Uncertainty Propagation Method for Robust Aerodynamic Design," *AIAA Journal*, vol. 49, 2011, pp. 530–543.
- [21] Guenov, M. D., Nunez, M., Molina-Cristóbal, A., Sripawadkul, V., Datta, V., and Riaz, A., "Composition, Management,

- and Exploration of Computational Studies at Early Design Stage,” *Computational Intelligence in Aerospace Sciences*, American Institute of Aeronautics and Astronautics, Inc., 2014, pp. 415–460.
- [22] McCullers, L. A., *Flight Optimization System*, NASA Langley Research Center, 2011.
- [23] Chakraborty, I., Trawick, D. R., Mavris, D. N., Emeneth, M., and Schneegans, A., “A Requirements-driven Methodology for Integrating Subsystem Architecture Sizing and Analysis into the Conceptual Aircraft Design Phase,” *14th AIAA Aviation Technology, Integration, and Operations Conference*, American Institute of Aeronautics and Astronautics, 2014.
- [24] Lammering, T., “Integration of Aircraft Systems into Conceptual Design Synthesis,” PhD thesis, RWTH Aachen University, 2014.
- [25] De Tenorio, C., “Methods for Collaborative Conceptual Design of Aircraft Power Architectures,” PhD thesis, Georgia Institute of Technology, 2010.
- [26] Shibata, K., Maedomari, T., Rinoie, K., Morioka, N., and Oyori, H., “Aircraft Secondary Power System Integration into Conceptual Design and Its Application to More Electric System,” *SAE 2014 Aerospace Systems and Technology Conference*, SAE International, 2014.
- [27] Xia, X., and Lawson, C. P., “The Development of a Design Methodology for Dynamic Power Distribution Management on a Civil Transport All Electric Aircraft,” *Aerospace Science and Technology*, vol. 25, 2013, pp. 125–131.
- [28] Cukier, R. I., Fortuin, C. M., Shuler, K. E., Petschek, A. G., and Schaibly, J. H., “Study of the Sensitivity of Coupled Reaction Systems to Uncertainties in Rate Coefficients. I Theory,” *The Journal of Chemical Physics*, vol. 59, 1973, pp. 3873–3878.
- [29] Sobol’, I. M., “On the Distribution of Points in a Cube and the Approximate Evaluation of Integrals,” *USSR Computational Mathematics and Mathematical Physics*, vol. 7, 1967, pp. 86–112.
- [30] Tarantola, S., Gatelli, D., and Mara, T. A., “Random Balance Designs for the Estimation of First Order Global Sensitivity Indices,” *Reliability Engineering & System Safety*, vol. 91, 2006, pp. 717–727.